Letter

Active buckling of pressurized spherical shells: Monte Carlo simulation

Vipin Agrawal [1,2,*] Vikash Pandey [1,†] and Dhrubaditya Mitra [1,‡]

[1] *Nordita, KTH Royal Institute of Technology and Stockholm University, Hannes Alfvéns väg 12, 106 91 Stockholm, Sweden*
[2] *Department of Physics, Stockholm University, AlbaNova University Centre, Fysikum, 106 91 Stockholm, Sweden*

We study the buckling of pressurized spherical shells by Monte Carlo simulations in which the detailed balance is explicitly broken—thereby driving the shell to be active, out of thermal equilibrium. Such a shell typically has either higher (active) or lower (sedate) fluctuations compared to one in thermal equilibrium depending on how the detailed balance is broken. We show that, for the same set of elastic parameters, a shell that is not buckled in thermal equilibrium can be buckled if turned active. Similarly a shell that is buckled in thermal equilibrium can unbuckle if sedated. Based on this result, we suggest that it is possible to experimentally design microscopic elastic shells whose buckling can be optically controlled.

Thin spherical shells are commonly found in many natural and engineering settings. Their sizes can vary over a very large range—from hundred meters, e.g., the Avicii Arena, Stockholm [1], down to about hundred nanometers, e.g., viral capsules [2,3] and exosomes [4,5]. The elastic properties of shells, including conditions under which buckling can occur, have been extensively studied [6–11]. Interest in this traditional field of applied mathematics has been rekindled in the past decades because of possible applications to biology and nanoscience [2,3,12–20]. For example, the elastic shell is used as a model for nuclear membrane [21]. Furthermore, the cell membrane, although often modeled simply as a fluid membrane, is dynamically tethered to the cytoskeleton—thereby acquiring effective in-plane elastic properties. For example, it has been shown [22] that to capture the stomatocyte-discocyte-echinocyte sequence of the human red blood cell within one unified model it is necessary to introduce nonlinear in-plane shear elastic modulus of the membrane. Numerical simulations of flowing red blood cells that faithfully reproduce experimental observations also must use nonlinear shear elastic modulus [23–28]. Crucially, it has been shown that for small enough shells the thermal fluctuations can bring down the critical buckling pressure by a large amount [29,30]. This opens up the intriguing possibility of how the elastic properties of shells, in particular buckling, will change if they are turned active—driven out of thermal equilibrium.

The fundamental property of living matter is that they are not in thermal equilibrium [31] even over timescales for which they are statistically stationary. They are active—they consume energy and generate entropy [32]. The statistical and mechanical properties of active matter is a current topic of considerable interest [33,34]. The fluctuations of the membranes of living cells have active components, in addition to the thermal fluctuations, due to, e.g., driving by the active cytoskeleton [35–39].

Thus, many cells can be considered active shells, although not spherical. Active shells can also be synthetically designed, e.g., by embedding certain proteins—proteins that acts as active pumps when irradiated with light of a certain frequency [40,41]. Shells made out of hard, magnetic elastomers can be turned active by an external fluctuating magnetic field [42]. Such shells cannot be described by equilibrium statistical mechanics.

In this Letter, we study the buckling of pressurized spherical shells using the Monte Carlo (MC) simulations [43] in which *detailed balance is explicitly broken*—thereby driving the shell to be active, out of thermal equilibrium. Such a shell typically has fluctuations that are either higher or lower those in thermal equilibrium depending on how the detailed balance is broken. We call such nonequilibrium stationary states *active* and *sedate*, respectively. We show that, within the right range of elastic parameters, a shell that is not buckled in thermal equilibrium can be buckled if turned active. Similarly a shell that is buckled in thermal equilibrium can unbuckle if turned sedate (see Fig. 1). Based on our study, we suggest that it is possible to experimentally design microscopic elastic shells whose buckling can be optically controlled.

Let us briefly summarize, following Refs. [29,30], the model and the key results of the theory of thin elastic shells in *thermal equilibrium*. A pressurized elastic shell is described by an effective Hamiltonian, $G_{\text{eff}} = G_0 + G_1$, where

$$G_0[f] = \frac{1}{2} \int d^2\boldsymbol{x} \left[B(\nabla^2 f)^2 - \frac{PR}{2} |\nabla f|^2 + \frac{Y}{R^2} f^2 \right] \quad \text{(1a)}$$

and

$$G_1[f] = \frac{Y}{2} \int d^2\boldsymbol{x} \left[\left(\frac{1}{2} \mathcal{P}_{ij} \partial_i f \partial_j f \right)^2 - \frac{f}{R} \mathcal{P}_{ij} \partial_i f \partial_j f \right]. \quad \text{(1b)}$$

*vipin.agrawal@su.se
†vikash.pandey@su.se
‡dhruba.mitra@gmail.com
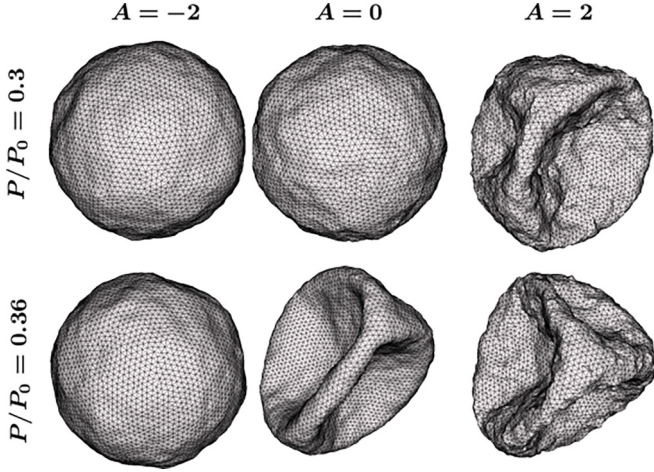
FIG. 1. Active buckling. Typical snapshots from our simulations for activity $A = -2$, 0, and 2 (from left to right) and pressure $P = 0.30 P_0$ (top row) and $0.36 P_0$ (bottom row), where P_0 is the critical buckling pressure obtained from the mechanical theory of elastic shells, i.e., at zero temperature. We use $N = 5120$, FvK = 4616, and ET = 8. The middle column, $A = 0$, corresponds to shells in thermal equilibrium—an unbuckled shell buckles upon increasing P/P_0 from 0.30 to 0.36. This is consistent with the results of Refs. [29,30]. Top row: As activity is increased to 2 (right column), the shell buckles. Bottom row: Whereas as activity is decreased to -2 (left column) the shell, that was buckled in thermal equilibrium does not buckle at the same pressure.

Here $\boldsymbol{x} = (x_1, x_2)$ is a two-dimensional Cartesian coordinate system and $\mathcal{P}_{ij} \equiv \delta_{ij} - \partial_i \partial_j / \nabla^2$ is the transverse projection operator. The out-of-plane displacement is $h(\boldsymbol{x}) = f_0(\boldsymbol{x}) + f(\boldsymbol{x})$, where $f_0(\boldsymbol{x})$ is the uniform contraction of the sphere in response to the external pressure. The difference between the external and the internal pressure is P. The part G_0 is harmonic and the part G_1 is anharmonic. In this model, we assume the shell to be amorphous and homogeneous with radius R, bending modulus B and (two-dimensional) Young's modulus Y. Two non-dimensional numbers determine the elastic behavior of such shells, the Föppl–von Karman number and the elastothermal number, defined respectively as

$$\text{FvK} \equiv \frac{YR^2}{B}, \quad \text{ET} \equiv \frac{k_B T}{B} \sqrt{\text{FvK}}, \quad (2)$$

where k_B is the Boltzmann constant and T is the temperature. At constant ET, the effects of anharmonicity increases with FvK, whereas at constant elastic modulii the effects of thermal fluctuations increase with ET. Ignoring the anharmonic contribution, using standard tools of equilibrium statistical mechanics it is straightforward [[29], Eq. 4] to calculate the spectrum of fluctuations:

$$S(\boldsymbol{q}) \equiv \langle \hat{f}(\boldsymbol{q}) \hat{f}(-\boldsymbol{q}) \rangle = \frac{k_B T}{a \left(Bq^4 - \frac{PRq^2}{2} + \frac{Y}{R^2} \right)}, \quad (3)$$

where $\hat{f}(\boldsymbol{q})$ is the Fourier transform of $f(\boldsymbol{x})$ and a is the area of integration in the (x_1, x_2) plane. In equilibrium, the symbol $\langle \cdot \rangle$ denotes thermal averaging; whereas for active cases, it denotes

averaging over the nonequilibrium stationary states. Note that $S(\boldsymbol{q})$ blows up for

$$P = P_0 \equiv \frac{4B}{R} q_*^2, \quad (4a)$$

where

$$q_* \equiv \left(\frac{Y}{BR^2} \right)^{1/4} = \frac{\text{FvK}^{1/4}}{R}, \quad (4b)$$

where P_0 is the buckling pressure, independent of temperature, obtained within the traditional theory [11] of buckling of pressurized shells. For a large Föppl–von Karman number, $q_* > 1/R$ is the buckling mode. Refs. [29,30] used renormalization group (RG) techniques to show that the effects of the anharmonic terms is to renormalize the parameters appearing in the bare theory, i.e., P, B, and Y in (3) must be replaced by their scale–dependent, renormalized versions, see Ref. [[30], Eq. 18]. Consequently both the pressure and the critical buckling pressure are renormalized and buckling is obtained if both of these quantities are equal for a length scale which must be smaller than the radius of the sphere [30]. The results of this RG analysis were validated by Monte Carlo simulations of spherical shell, randomly triangulated with N grid points, with discretized bending and stretching energies that translate directly into a macroscopic elastic modulii [29,44,45]. Our Monte Carlo code, described in detail in Ref. [46], closely follows that of Ref. [29], and faithfully reproduces these results (see Supplemental Material [47]). We incorporate activity into this model in the following manner.

Over the years, many theoretical models [48–54] have been suggested to incorporate the effects of active fluctuations into models of membranes. We use a method that is well suited to use the Monte Carlo setup and has been used before to study Ising models out of equilibrium [43,55–57]—the idea is to break detailed balance while preserving stationarity. In equilibrium Monte Carlo simulations two common choices of the transition rate from one state to another are the Metropolis (W_{Met}) and the Glauber (W_{Gla}), given respectively by

$$W_{\text{Met}} = \min \left[1, \exp \left(-\frac{E}{k_B T} \right) \right] \quad (5a)$$

and

$$W_{\text{Gla}} = \frac{1}{2} \left[1 - \tanh \left(\frac{E}{2k_B T} \right) \right], \quad (5b)$$

where k_B is the Boltzmann constant, T is the temperature, and E is the difference in energy between the two states. To drive the membrane out of equilibrium, following Ref. [43], we replace E by $E + \Delta E$, where ΔE is a constant. This guarantees that detailed balance is broken and the amount by which it is broken is ΔE. If ΔE is positive (negative), the probability of acceptance of large fluctuations is decreased (increased). Thus, we define a dimensionless quantity $A = -\Delta E/(k_B T)$ such that simulations with positive A, *active* simulations, have fluctuations higher than those of equilibrium ones, whereas for negative A, *sedate* simulations, the fluctuations are less than the equilibrium ones. For most of the simulations reported here, we use the Metropolis algorithm. In some representative cases, for both equilibrium and
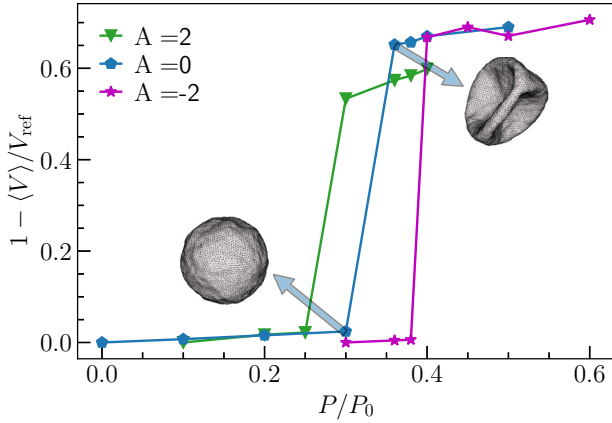
FIG. 2. Buckling under pressure. Normalized change in volume as a function of external pressure for (blue) a shell in thermal equilibrium, (green) active ($A = 2$), and (magenta) sedate ($A = -2$) for simulations with ET = 8, FvK = 4616, and the number of grid points $N = 5120$. Here $\langle V \rangle$ is the ensemble average of volume, and V_{ref} is the average volume at the smallest pressure difference. The error in $\langle V \rangle$ are the shades around the solid lines—they are too small to be visible. The signature of buckling is the sudden large change in volume. The critical buckling pressure for the thermal case is consistent with Refs [29,30].

nonequilibrium simulations, we have checked that both the Glauber and Metropolis algorithms give the same result.

For lipid vesicles in thermal equilibrium, standard techniques of equilibrium statistical mechanics [38] and micropipet aspiration experiments show $\Delta \alpha \propto (k_B T / 4 \pi B) \ln \sigma$, where $\Delta \alpha$ is the areal strain and σ is the surface tension. For active membranes the same proportionality holds, but the constant of proportionality is different [41]. This experimental result was captured by the model in Ref. [58], which adds an additional Ornstein-Uhlenbeck noise to the models of thermal membranes. Our active Monte Carlo scheme, in planar membranes [59], reproduces the results of Ref. [58] and also the experimental result of Ref. [41].

In summary, we incorporate the technique of active Monte Carlo [43] into the Monte Carlo algorithm for spherical shells in thermal equilibrium [29,44,46] to simulate active shells.

In Fig. 2 we show a typical plot of how the volume V of the spherical shell changes as the external pressure is increased from a very small value. The simulations are done in a constant pressure ensemble, and hence, volume is a fluctuating quantity. Henceforth, by volume we mean the average volume $\langle V \rangle$. The average volume at the smallest pressure difference is the reference volume V_{ref}. The error in $\langle V \rangle$, shown by the shaded regions in Fig. 2, are the variances—they are too minute to be visible. First consider the shell under thermal equilibrium. Buckling shows up as a sharp decrease in volume accompanied by a typical buckled shape, as shown in Fig. 1. The critical buckling pressure P_c that we obtain is consistent with the results of Refs. [29,30]. We show the results of the simulations for both the active, $A = 2$, and the sedate, $A = -2$, cases. For the former the critical buckling pressure decreases, while for the latter the critical buckling pressure increases.

Next we decompose the fluctuating height field $f(\theta, \phi)$ in spherical harmonics $\mathcal{Y}_{\ell,m}(\theta, \phi)$:

$$f(\theta, \phi) = \sum_{\ell,m} \tilde{f}_{\ell,m} \mathcal{Y}_\ell^m(\theta, \phi), \tag{6a}$$

and we define

$$S(\ell) = \frac{4\pi}{(2\ell + 1)|\tilde{f}_{00}|^2} \sum_{m=-\ell}^{\ell} |\tilde{f}_{\ell,m}|^2. \tag{6b}$$

In the Supplemental Material [47], we compare typical plots of $S(\ell)$ for buckled and unbuckled shells. Buckling is accompanied by the appearance of a peak in $S(\ell)$ at a small ℓ value. For the equilibrium case, buckling as a function of external pressure is an equilibrium phase transition with the amplitude of the peak of $S(\ell)$ at small ℓ as the order parameter [29]. However, buckling at the fixed P and ET as a function of activity is not an equilibrium phase transition, but can be considered as a dynamical one. Nevertheless, we can still characterize buckling by the appearance of a peak in $S(\ell)$ for small ℓ.

To obtain the phase diagram we use 13 values of the elastothermal number, for each of which we use 7 values of activity. For a fixed choice of elastothermal number and activity, we start our simulations with an initial condition where the shell is a perfect sphere. Then we choose a fixed value of external pressure and run our simulations till we reach a stationary state, which for zero activity is the equilibrium state. Whether the shell is buckled or not is decided by three checks: (a) significant decrease of volume, (b) a peak at small ℓ for $S(\ell)$, and (c) visual inspection. If the shell is not buckled we choose a higher external pressure and start our simulations again from the same initial condition. The buckling pressure P_c obtained for a set of parameters is given in the Supplemental Material [47]. This way we mark out the phase boundary in the pressure–elastothermal number plane for different activities and in the pressure-activity plane for different elastothermal numbers (see Fig. 3). In Fig. 3(a) we also plot the phase boundary, obtained through a RG calculation in Ref. [30], which agrees reasonably well with our numerical results for zero activity. Note that for large enough values of ET and A we reach a part of the phase diagram where the shell is unstable at zero external pressure and can be made stable only with positive internal pressure. This part of the phase diagram is not shown in Fig. 3, although the relevant data are included in the Supplemental Material [47]. Note that at small ET for the sedate case it is possible to have the shell remain unbuckled ever for pressures higher than P_0; i.e., the shell is stabilized.

Several comments are now in order. One, most of our simulations use $N = 5120$. We have repeated some of our simulations with $N = 20\,252$ and obtained the same buckling pressure. Two, to obtain the buckling pressure we always start from the same initial condition and imposed a fixed external pressure. Hence, the lines of phase separation we show (Fig. 3) are not continuous and will be improved if the phase diagram is sampled in a finer resolution. Three, experimentally, it is unclear how to implement the sedate regime, negative A. Nevertheless, synthetic membranes that can be turned active ($A > 0$) optically have been already realized by embedding certain proteins in bi-lipid membranes—proteins that act
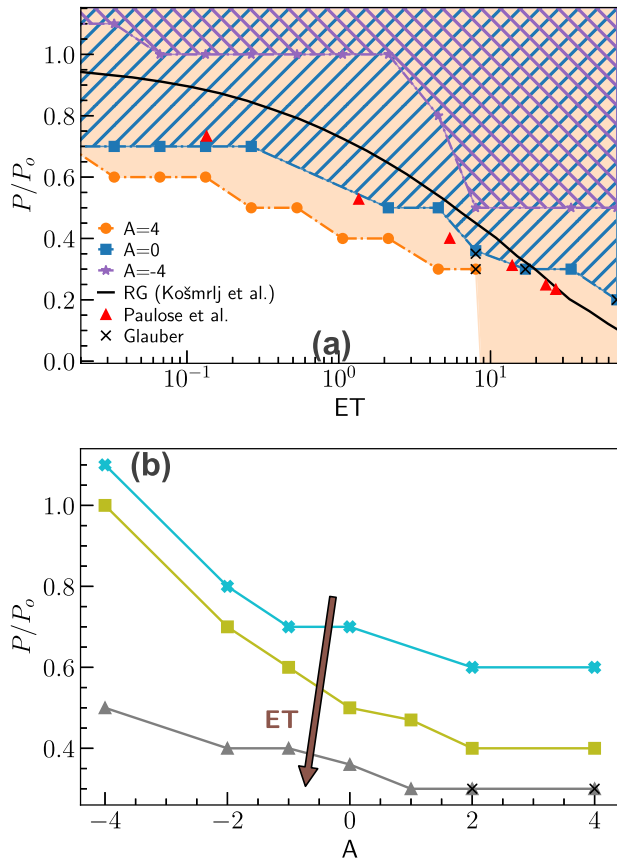
FIG. 3. Phase diagram. The phase boundary (a) in the pressure-elastothermal number plane for different activities and (b) in the pressure-activity plane for different elastothermal numbers (gray triangles for ET = 7.99, olive squares for ET = 2.12, and cyan cross for ET = 0.03). In panel (a) the region where the buckled phase is obtained in equilibrium is marked by blue lines. The region where the buckled phase is obtained for $A = 4$ is shaded in light yellow. The region where the buckled phase is obtained for $A = -4$ is marked by violet lines. Cases marked with a cross use the Glauber algorithm. In panel (a), the phase boundary obtained by RG calculation [30] is marked by a black line and the simulation results from Ref. [29] are represented by red triangles.

critical buckling pressure changes as we change the fraction of active points. Four, bilipid membranes are semipermeable [60]. As the shell buckles the fraction of solute increases, increasing the partial pressure inside the shell. Experimentally, this can be avoided by using shells with holes in them. We expect, in such cases, the buckling pressure may change by a small amount. Five, as there are many different models of active elastic material, it behooves us to study the universality of our result by performing similar simulations in other models. This is outside the scope of the present work. Six, note that the parameter A signifies the breakdown of detailed balance. It is not a quantity that can be directly measured experimentally. However, breakdown of detailed balance implies that the system is not in equilibrium. Hence, in a statistically stationary state the system will show entropy production. The rate of entropy generation, calculated from the fluctuations of the shell, may act as an indirect measure of activity A.

Finally, our simulations point towards the intriguing possibility that, within the right range of elastic parameters, a shell that is not buckled in thermal equilibrium can be buckled if turned optically active. Based on this, we suggest that it is possible to experimentally design microscopic elastic shells whose buckling can be optically controlled. In such devices it may be possible to drive flows at microscopic scales by the buckling and unbuckling of shells, optically.

as active pumps when irradiated with light of a certain frequency [40,41]. In such cases, only a fraction of points on the shell are active. This can be incorporated in a straightforward manner in our code and it would be interesting to see how the

[1] There are several geodesic domes with sizes ranging from 10 to 200 m.

[2] M. Buenemann and P. Lenz, Elastic properties and mechanical stability of chiral and filled viral capsids, Phys. Rev. E **78**, 051924 (2008).

[3] J. P. Michel, I. L. Ivanovska, M. M. Gibbons, W. S. Klug, C. M. Knobler, G. J. L. Wuite, and C. F. Schmidt, Nanoindentation studies of full and empty viral capsids and the effects of capsid protein mutations on elasticity and strength, Proc. Natl. Acad. Sci. USA **103**, 6184 (2006).

[4] D. M. Pegtel and S. J. Gould, Exosomes, Annu. Rev. Biochem. **88**, 487 (2019).

[5] S. Cavallaro, J. Horak, P. Haag, D. Gupta, C. Stiller, S. S. Sahu, A. Gorgens, H. K. Gatty, K. Viktorsson, S. El Andaloussi *et al.*, Label-free surface protein profiling of extracellular vesicles by an electrokinetic sensor, ACS Sensors **4**, 1399 (2019).

[6] A. E. H. Love, *A Treatise on the Mathematical Theory of Elasticity*, 4th ed. (Dover, New York, 2011).

[7] L. D. Landau and E. M. Lifshitz, *Theory of Elasticity*, Course of Theoretical Physics Vol. 7 (Pergamon, Oxford, England, 1970).

[8] W. T. Koiter, *Progress in Applied Mechanics (The Prager Anniversary Volume)* (Macmillan, New York, 1963).

[9] W. T. Koiter, Current trends in theory of buckling, in *Buckling of Structures: Symposium Cambridge/USA*, edited by B. Budiansky (Springer-Verlag, Berlin, 1976), pp. 1–16.

[10] A. V. Pogorelov, *Bendings of Surfaces and Stability of Shells* Vol. 72 (American Mathematical Society, Providence, 1988).

[11] J. W. Hutchinson, Buckling of spherical shells revisited, Proc. R. Soc. London, Ser. A **472**, 20160577 (2016).

[12] G. A. Vliegenthart and G. Gompper, Mechanical deformation of spherical viruses with icosahedral symmetry, Biophys. J. **91**, 834 (2006).

[13] C. Gao, E. Donath, S. Moya, V. Dudnik, and H. Möhwald, Elasticity of hollow polyelectrolyte capsules prepared by the layer-by-layer technique, Eur. Phys. J. E **5**, 21 (2001).

[14] V. D. Gordon, X. Chen, J. W. Hutchinson, A. R. Bausch, M. Marquez, and D. A. Weitz, Self-assembled polymer membrane capsules inflated by osmotic pressure, J. Am. Chem. Soc. **126**, 14117 (2004).

[15] D. Vella, A. Ajdari, A. Vaziri, and A. Boudaoud, The indentation of pressurized elastic shells: From polymeric capsules to yeast cells, J. R. Soc., Interface **9**, 448 (2012).

[16] D. Vorselen, F. C. MacKintosh, W. H. Roos, and G. J. L. Wuite, Competition between bending and internal pressure governs the mechanics of fluid nanovesicles, ACS Nano **11**, 2628 (2017).

[17] P.-H. Wu, D. R.-B. Aroush, A. Asnacios, W.-C. Chen, M. E. Dokukin, B. L. Doss, P. Durand-Smet, A. Ekpenyong, J. Guck, N. V. Guz *et al.*, A comparison of methods to assess cell mechanical properties, Nat. Methods **15**, 491 (2018).

[18] D. Vorselen, M. C. Piontek, W. H. Roos, and G. J. L. Wuite, Mechanical characterization of liposomes and extracellular vesicles, a protocol, Front. Mol. Biosci. **7**, 139 (2020).

[19] S. Cavallaro, F. Pevere, F. Stridfeldt, A. Görgens, C. Paba, S. S. Sahu, D. R. Mamand, D. Gupta, S. El Andaloussi, J. Linnros *et al.*, Multiparametric profiling of single nanoscale extracellular vesicles by combined atomic force and fluorescence microscopy: correlation and heterogeneity in their molecular and biophysical features, Small **17**, 2008155 (2021).

[20] C. I. Zoldesi, I. L. Ivanovska, C. Quilliet, G. J. L. Wuite, and A. Imhof, Elastic properties of hollow colloidal particles, Phys. Rev. E **78**, 051401 (2008).

[21] J. A. Jackson, N. Romeo, A. Mietke, K. J. Burns, J. F. Totz, A. C. Martin, J. Dunkel, and J. I. Alsous, Dynamics, scaling behavior, and control of nuclear wrinkling, arXiv:2210.11581.

[22] G. L. HW, M. Wortis, and R. Mukhopadhyay, Stomatocyte–discocyte–echinocyte sequence of the human red blood cell: Evidence for the bilayer–couple hypothesis from membrane mechanics, Proc. Natl. Acad. Sci. USA **99**, 16766 (2002).

[23] D. A. Fedosov, B. Caswell, and G. Em Karniadakis, A multiscale red blood cell model with accurate mechanics, rheology, and dynamics, Biophys. J. **98**, 2215 (2010).

[24] D. A. Fedosov, B. Caswell, and G. Em Karniadakis, Systematic coarse-graining of spectrin-level red blood cell models, Comput. Methods Appl. Mech. Eng. **199**, 1937 (2010).

[25] D. A. Fedosov, Multiscale modeling of blood flow and soft matter, Ph.D. thesis, Division of Applied Mathematics at Brown University, 2010.

[26] D. A. Fedosov, W. Pan, B. Caswell, G. Gompper, and G. E. Karniadakis, Predicting human blood viscosity in silico, Proc. Natl. Acad. Sci. USA **108**, 11772 (2011).

[27] J. B. Freund, Numerical simulation of flowing blood cells, Annu. Rev. Fluid Mech. **46**, 67 (2014).

[28] L. Zhu, C. Rorai, D. Mitra, and L. Brandt, A microfluidic device to sort capsules by deformability: A numerical study, Soft Matter **10**, 7705 (2014).

[29] J. Paulose, G. A. Vliegenthart, G. Gompper, and D. R. Nelson, Fluctuating shells under pressure, Proc. Natl. Acad. Sci. USA **109**, 19551 (2012).

[30] A. Košmrlj and D. R. Nelson, Statistical Mechanics of Thin Spherical Shells, Phys. Rev. X **7**, 011002 (2017).

[31] E. Schrödinger, *What is life?: With Mind and Matter and Autobiographical Sketches* (Cambridge University, Cambridge, England, 2012).

[32] F. S. Gnesotto, F. Mura, J. Gladrow, and C. P. Broedersz, Broken detailed balance and non-equilibrium dynamics in living systems: A review, Rep. Prog. Phys. **81**, 066601 (2018).

[33] M. C. Marchetti, J. F. Joanny, S. Ramaswamy, T. B. Liverpool, J. Prost, M. Rao, and R. A. Simha, Hydrodynamics of soft active matter, Rev. Mod. Phys. **85**, 1143 (2013).

[34] S. Ramaswamy, The mechanics and statistics of active matter, Annu. Rev. Condens. Matter Phys. **1**, 323 (2010).

[35] Z. Peng, X. Li, I. V. Pivkin, M. Dao, G. E. Karniadakis, and S. Suresh, Lipid bilayer and cytoskeletal interactions in a red blood cell, Proc. Natl. Acad. Sci. USA **110**, 13356 (2013).

[36] H. Turlier, D. A. Fedosov, B. Audoly, T. Auth, N. S. Gov, C. Sykes, J.-F. Joanny, G. Gompper, and T. Betz, Equilibrium physics breakdown reveals the active nature of red blood cell flickering, Nat. Phys. **12**, 513 (2016).

[37] A. Biswas, A. Alex, and B. Sinha, Mapping cell membrane fluctuations reveals their active regulation and transient heterogeneities, Biophys. J. **113**, 1768 (2017).

[38] H. Turlier and T. Betz, Unveiling the active nature of living-membrane fluctuations and mechanics, Annu. Rev. Condens. Matter Phys. **10**, 213 (2019).

[39] S. K. Manikandan, T. Ghosh, T. Mandal, A. Biswas, B. Sinha, and D. Mitra, Estimate of entropy generation rate can spatiotemporally resolve the active nature of cell flickering, arXiv:2205.12849.

[40] P. Girard, J. Prost, and P. Bassereau, Passive or Active Fluctuations in Membranes Containing Proteins, Phys. Rev. Lett. **94**, 088102 (2005).

[41] J.-B. Manneville, P. Bassereau, S. Ramaswamy, and J. Prost, Active membrane fluctuations studied by micropipet aspiration, Phys. Rev. E **64**, 021908 (2001).

[42] D. Yan, M. Pezzulla, L. Cruveiller, A. Abbasi, and P. M. Reis, Magneto-active elastic shells with tunable buckling strength, Nat. Commun. **12**, 2831 (2021).

[43] M. Kumar and C. Dasgupta, Nonequilibrium phase transition in an Ising model without detailed balance, Phys. Rev. E **102**, 052111 (2020).

[44] G. Gompper and D. M. Kroll, Triangulated-surface models of fluctuating membranes, in *Statistical Mechanics of Membranes and Surfaces*, edited by D. Nelson, T. Piran, and S. Weinberg (World Scientific, Singapore, 2004), pp. 359–426.

[45] C. Itzykson, in *Proceedings of the GIFT Seminar, Jaca 85*, edited by J. Abad *et al.* (World Scientific, Singapore, 1986), pp. 130–188.

[46] V. Agrawal, V. Pandey, H. Kylhammar, A. Dev, and D. Mitra, MeMC: A package for Monte Carlo simulations of spherical shells, J. Open Source Software **7**, 4305 (2022).

[47] See Supplemental Material at http://link.aps.org/supplemental/10.1103/PhysRevE.108.L032601 for (a) details of the algorithm we use in our simulations; (b) benchmark with earlier simulations; and (c) additional figures.

[48] S. Ramaswamy, J. Toner, and J. Prost, Nonequilibrium Fluctuations, Traveling Waves, and Instabilities in Active Membranes, Phys. Rev. Lett. **84**, 3494 (2000).

[49] M. Rao and Sarasij R. C., Active Fusion and Fission Processes on a Fluid Membrane, Phys. Rev. Lett. **87**, 128101 (2001).

[50] B. Loubet, U. Seifert, and M. A. Lomholt, Effective tension and fluctuations in active membranes, Phys. Rev. E **85**, 031913 (2012).

[51] A. Maitra, P. Srivastava, M. Rao, and S. Ramaswamy, Activating Membranes, Phys. Rev. Lett. **112**, 258101 (2014).

[52] R. J. Hawkins and T. B. Liverpool, Stress Reorganization and Response in Active Solids, Phys. Rev. Lett. **113**, 028102 (2014).

[53] S. Yin, B. Li, and X.-Q. Feng, Bio-chemo-mechanical theory of active shells, J. Mech. Phys. Solids **152**, 104419 (2021).

[54] A. Goriely, Five ways to model active processes in elastic solids: active forces, active stresses, active strains, active fibers, and active metrics, Mech. Res. Commun. **93**, 75 (2017).

[55] H. Künsch, Nonreversible stationary measures for infinite interacting particle systems, Z. Wahrscheinlichkeitstheorie Verw. Geb. **66**, 407 (1984).

[56] C. Godreche and A. J. Bray, Nonequilibrium stationary states and phase transitions in directed ising models, J. Stat. Mech.: Theory Exp. (2009) P12016.

[57] C. Godrèche, Rates for irreversible Gibbsian Ising models, J. Stat. Mech.: Theory Exp. (2013) P05011.

[58] J. Prost and R. Bruinsma, Shape fluctuations of active membranes, Europhys. Lett. **33**, 321 (1996).

[59] A. Fragkiadoulakis, S. K. Manikandan, and D. Mitra (unpublished).

[60] R. Phillips, J. Kondev, J. Theriot, H. G. Garcia, and N. Orme, *Physical Biology of the Cell* (Garland Science, London, 2012).

[61] V. Agrawal, https://github.com/vipinagrawal25/MeMC/releases/tag/v1.1.

[62] Zenodo, doi: 10.5281/zenodo.6772570.

[63] M. Caroli, P. M. M. de Castro, S. Loriot, O. Rouiller, M. Teillaud, and C. Wormser, Robust and efficient Delaunay triangulations of points on or close to a sphere, in *International Symposium on Experimental Algorithms* (Springer, Berlin, 2010), pp. 462–473.

[64] A simple and fast mesh generator, https://github.com/meshpro/meshzoo.

[65] J. D. Hunter, Matplotlib: A 2d graphics environment, Comput. Sci. Eng. **9**, 90 (2007).

[66] H. Childs, E. Brugger, B. Whitlock, J. Meredith, S. Ahern, D. Pugmire, K. Biagas, M. Miller, C. Harrison, G. H. Weber, H. Krishnan, T. Fogal, A. Sanderson, C. Garth, E. Wes Bethel, D. Camp, O. Rübel, M. Durant, J. M. Favre, and P. Navrátil, VisIt: An end-user tool for visualizing and analyzing very large data, in *High Performance Visualization–Enabling Extreme-Scale Scientific Insight*, edited by E. Wes Bethel, H. Childs, and C. Hansen (CRC, Boca Raton, FL, 2012), pp. 357–372.